

RESEARCH ARTICLE

The Weak Soil Investigation at The Slope Zone in The Hot Spring Area, Rokan Hulu, Indonesia

¹Nur Islami

¹Physics PMIPA, Universitas Riau, Jl. HR. Soebrantas, Pekanbaru, 28293, Indonesia

Corresponding author: nurislami@lecturer.unri.ac.id
Tel.: +6281363888549
Received: Jul 1, 2019; Accepted: Aug 28, 2019.
DOI: 10.25299/jgeet.2019.4.4.4258

Abstract

The slope failure can occur due to the soil on the slope area is relatively porous and the surface water is easily to move in the soil. The zone of the weak zone of the soil should be detected early to avoid the ground mass movement on the slope area. This study is to investigate the weak zone of the soil on the slope area of the hot spring tourism location using geoelectrical resistivity and soil property analysis methods. The Wenner configuration with a total of 40 electrodes has been employed at each four resistivity survey lines. The electrode spacing was adjusted to be 2 – 5 meter in order to get relatively higher resolution of the resistivity data. Soil samples were collected at several site to measure the soil characteristics of the study area. The soil analysis results show that the study area consist of gravel, sand, clay, silt and weathered metasediment. The geoelectrical resistivity model shows the relatively low resistivity value of about 30 ohm.m at the slope zone which is indicating that the soil has higher porosity. Generally only a few locations with the weak soil zone detected in the slope of the hot spring area, however, it is not potential for the ground mass movement due to the soil is relatively thin.

Keywords: Geoelectrical Resistivity, Rokan Hulu, Slope Failure, Soil

1. Introduction

In the undulation ground zones, the mass movement are often becoming a disaster that can cause loss of the wealth and threat the safety of the human (Federico et al., 2018). Landslides are a type of natural disaster that often occurs in Indonesia. Generally, the movement between plates in the subduction zones causes the ground surface morphology varies from lowland to high mountains (Satoru et al., 2015). Furthermore, as a country on the equator, Indonesia has climatological conditions with high rainfall. High rainfall can soften the soil which can cause dynamic forces resulting in slope instability (Shuai et al., 2016).

The study of landslide has been conducted using various method in the worldwide. Zbigniew (2018) identified the landslide triggers by the 'nearly real-time' observing methods in the Carpathian Mountains. This area is one of the largest landslide zones in Europe. Jie et al., 2018, detected and characterized the displacement of the landslides by employing multi temporal satellite, in the Dadu River, Danba County. The research shown the potential landslides are detected from the several sites. They suggested the guidelines on InSAR applied in the study area. The successive landslide of dam formation has been analysed using dissimilar triggering mechanisms in Tangjiawan landslide, China (Xuanmei et al., 2018). The high intensity of earthquakes and great typical uplifting rate were inferred as the contribution of succeeding damming events. The runout simulations (Margherita et al., 2018) was used to investigate the Cima Salti landslide in Italy. In their research, the landslide was predicted travelled transversely motionless ice throughout the Lateglacial period.

Then, the simulations were used as an instrument in predicting valley growth and also the natural risks.

Geoelectrical resistivity method has been used widely to investigate the subsurface condition. The geoelectrical resistivity method was also can be used to detect the thickness of the peat soil and to predict the potential of groundwater resources in the coastal area (Islami et al., 2018a). The method was successfully employed to investigate the heavy metal zone in the groundwater system. The zone of heavy metal can be delianiated and mapped using this method (Islami et al., 2018b). The geoelectrical resistivity also was success to monitor the nitrate in the the shallow depth at the sandy soil area (Islami, 2017). The nitrate movement direction was clearly seen when it observed using the time lapse geoelectrical resistivity monitoring.

In this research, the use of geoelectrical resistivity and combined with the soil analysis method were used to investigate the weak soil zone in the Hot Spring tourism area of Rokan Hulu, Indonesia.

The interpretation of geoelectrical resistivity model was improved by the direct resistivity measurement and soil analysis result, so that the weak zone of the soil in the slope area can be detected well.

2. The Study Area

The study area is located in the Hot Spring tourism location, Rokan Hulu, Indonesia. The study area is mainly surrounded by the thick secondary forest. Figure 1 shows the location of study area that was obtained from Google Earth. In the figure, the thick secondary forest is clearly surrounding the pool of Hot Spring. The secondary thick forest situation can be seen in the Fig. 1 (bottom).

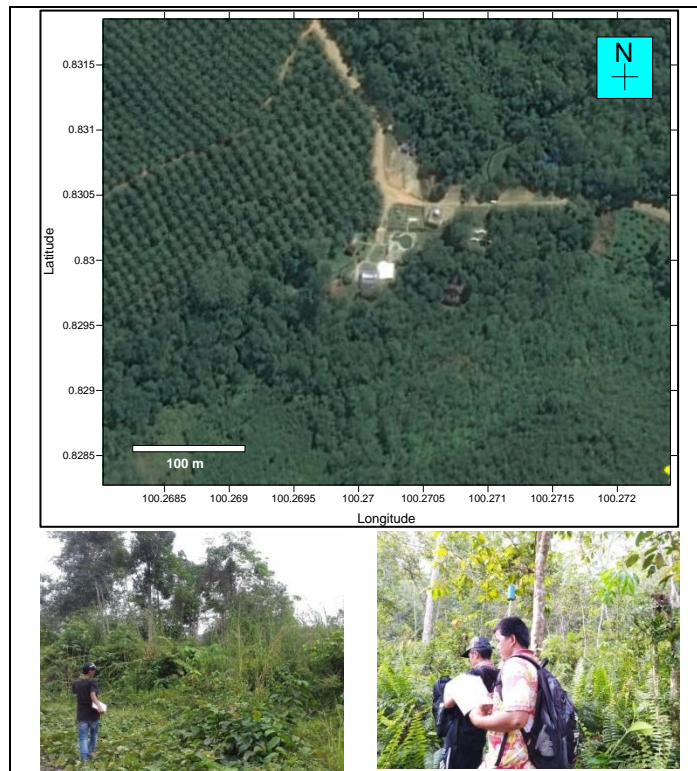


Fig. 1. The google map and the situation in the study area.

The study area consists of the Sihapas formation. The Sihapas formation comprising carbonaceous shale, clean quartz sandstones, conglomerate, and siltstones. The Telisa formation also can be found in the study area. It is containing of silty sandstone, calcareous to carbonaceous siltstones, and shale. A very massive intrusion is also found in the study area such consists of a cassiterite-bearing intrusion, granites, and also some granodiorites with zones of cataclasis. The age of intrusions are predicted of around the Jurassic zone. The intrusion are bring into being about 2.2 km after the hot spring to the south east path (Rock et al., 1983).

3. Methodology

The combination of three methods have been employed in this research. They were the geoelectrical resistivity survey, direct surface resistivity measurement and soil property analysis methods.

3.1. Geoelectrical resistivity survey

The geoelectrical resistivity survey was used in this research. Four lines of two dimension of geoelectrical resistivity with the Wenner configuration was employed for each survey lines. The home-made resistivity equipment was used in the survey. The total data reading for each line is 190 data which the reading was measure until the twelve layer measurement ($n=12$). The geoelectrical resistivity data then processed using the Res2Dinv software. In this software the real resistivity data was obtained and calculated based on the model that is built based on the measured data (Geotomo, 2007).

Fig. 2 is the design of the geoelectrical resistivity survey. For the each survey line, the first measurement was conducted for the first layer data ($n=1$), which is the electrode spacing is equal to a . Then, the second layer measurement is the second layer data ($n=2$). The measurement was continued until the twelve layer ($n=12$).

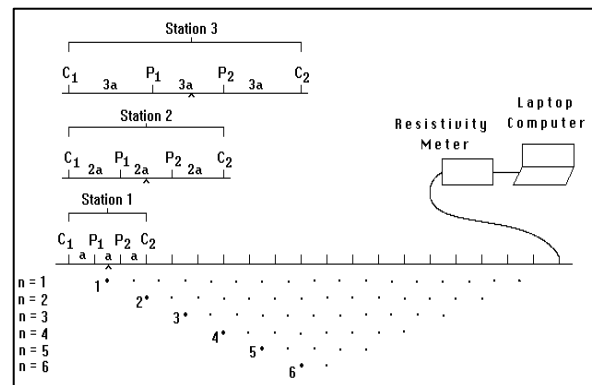


Fig. 2. The design of geoelectrical resistivity measurement. In this figure, total of the electrode is 19 with the n equal to 6 (adapted from Geotomo, 2017)

3.2. Surface direct resistivity measurement

Direct resistivity measurement on the surface with small electrode spacing was used for the improvement of the resistivity interpretation. This measurements were done in several sites with certain soil and rock condition. The data from these measurement were used to help in the geoelectrical resistivity model interpretation.

3.3 Grain size soil analysis

Soil samples were obtained from several location in the study area, especially at the location where the direct surface resistivity measurement was done. The soil was taken using hand auger if the target of the soil was at the depth more than 20 cm. The soil sample then dried and measure it grain size distribution and grouped based on gravel, sand, clay and silt.

4. Result and Discussion

4.1 The morphology of the study area

Fig. 3 shows the contour map of the study area. In the figure, it is clearly seen that the hot spring is situated on the surface of about 82 m above sea level. The hot spring is surrounded by the hill at the south part, the slope is relatively steep.

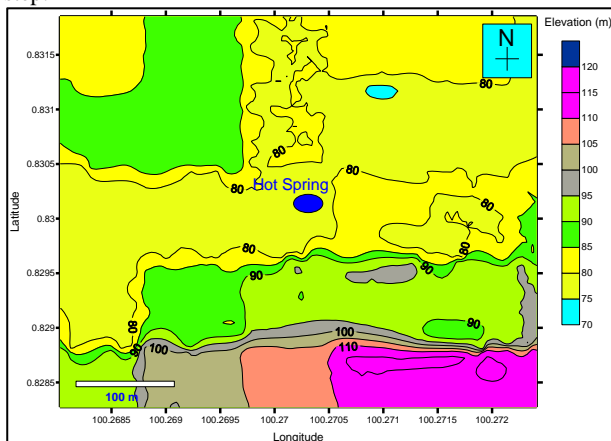


Fig. 3. The elevation contour of the study area

As seen in Fig 4, the hot spring is situated at the lower part of the hill. The hill should be assessed in term of the possibility of it weak zone. It is very important as the hot spring is very attracting the domestic tourist.

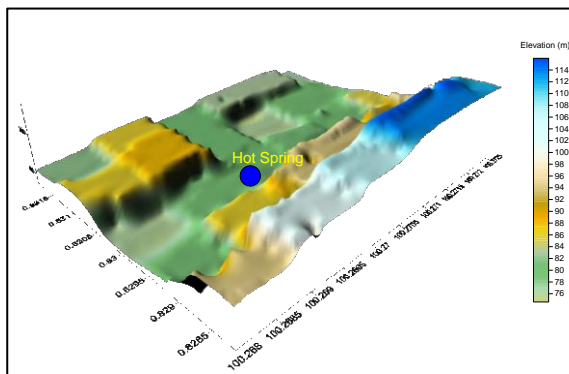


Fig. 4. The 3D shape of study area

4.2 Geoelectrical resistivity survey

The map of the resistivity survey location can be found in the Fig. 5. A total number of four resistivity survey was conducted on the slope zone of the hill at the south and north side of the hot spring location. In the map, the line survey is indicated with the line colour yellow. The survey was conducted at the thick secondary forest with relatively steep of the slope gradient.



Fig. 5. The geoelectrical resistivity survey location In the.

The result of geoelectrical resistivity survey model is given in the Fig 6. Fig. 6, the resistivity value for all resistivity line survey has the range of about 60 ohm.m until more than 3000 ohm.m. This is indicating the subsurface consists of a wide range of resistivity value. The resistive material such as methasediment can be predicted occur at the subsurface such as in Res Line 2, Res Line 3. The dark colour of brown-red is indicating the resistive material. However, on the surface at the several zone, the higher resistivity is also appeared. These value, besides the hard rock material, it is also possible due to the occurrence of the dried soil. In the Line 4, it can be seen that relatively low resistivity value can be observed at the surface, while the higher resistivity value of more than 3000 ohm.m can be found at the depth of 4 meter below the surface. This value may indicate that the hard rock is available at the depth

4.3. Direct resistivity measurement

Table 1 is the direct resistivity data measurement that was obtained from the selected surface at the study area. The measurement was done with 5 cm electrode spacing to make sure that the soil is homogeneous. Consequently the amount gotten is the real resistivity value with assumption that inside a range of 5 cm, the measured material is similar (Telford et al., 1990). Table 1 displays that comparative dry soil has an average resistivity of 562.1ohm.m. The medium when saturated by water, the soil resistivity declines vividly to 83.7ohm.m. The fresh methasediment has resistivity value of 3286.1 ohm.m on average. Whereas it is in wet condition, the resistivity become 1632.6ohm.m. Based on these data, the zone with the relatively higher water content will be ranging from 28.7-168.3 ohm.m.

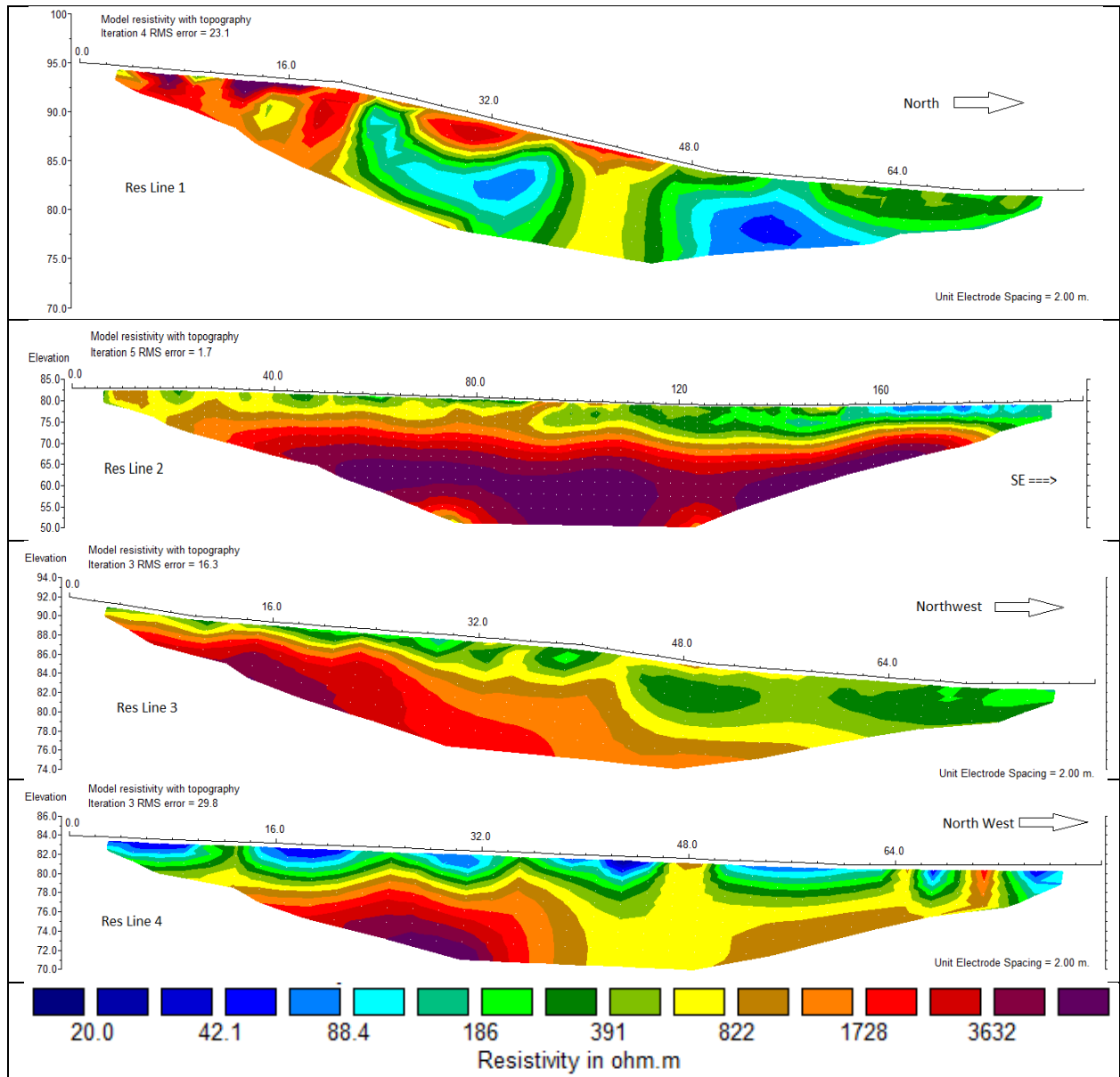


Fig. 6. Geoelectrical Resistivity model of Line 1, Line 2, line 3 and Line 4

Table 1. Direct resistivity measurement for small electrode spacing

| Material | Number of samples | Range of resistivity (ohm.m) | Average resistivity (ohm.m) |
|-------------------------|-------------------|------------------------------|-----------------------------|
| Dried soil (relatively) | 8 | 310.8-896.6 | 562.1 |
| Water-filled soil | 8 | 28.7-168.3 | 83.7 |
| Fresh methasediment | 8 | 2621.5-4328.5 | 3286.1 |
| Wet methasediment | 8 | 1376.2-3842.3 | 1632.6 |

4.4 Soil grain size distribution

Table 1 shows the grain size distribution of the soil sample in the study area. The soil sample was taken at the interested zone. The interested zone was defined from the result of resistivity survey. The soil sample was taken mainly in the low resistivity value in the geoelectrical resistivity survey.

Based on the data given in the table 1, there is no specific trend can be recorded. However, in the low resistivity zone, the sand content is relatively higher if compare to the another location.

The resistivity survey was conducted where the rainfall occur at the night before the survey. So that why the resistivity value at the higher sand content resulting the relatively low resistivity value.

Table 2. Grain size soil distribution obtained from the surface and depth of less than 1 m

| Sample ID | Latitude | Longitude | Depth (cm) | Gravel (%) | Sand (%) | Clay and Silt (%) |
|-----------|-----------|-----------|------------|------------|----------|-------------------|
| Soil - 01 | 0.8291051 | 100.26992 | 0 | 0 | 26.2 | 73.8 |
| Soil - 02 | 0.8296326 | 100.26996 | 15 | 0 | 23.1 | 76.9 |
| Soil - 03 | 0.8306599 | 100.27042 | 40 | 1.2 | 32.1 | 66.7 |
| Soil - 04 | 0.8297298 | 100.27044 | 60 | 2.5 | 31.4 | 66.1 |
| Soil - 05 | 0.8294105 | 100.27077 | 15 | 2.1 | 30.9 | 67.0 |
| Soil - 06 | 0.8296326 | 100.27146 | 80 | 4.2 | 32.1 | 63.7 |
| Soil - 07 | 0.8298407 | 100.27123 | 40 | 4.1 | 32.2 | 63.7 |

4.5 The weak soil zone on the slope area

Based on the geoelectrical resistivity data in Fig. 6, and supported by direct surface resistivity measurement in Table 1, and grain size distribution in Table 2, the weak soil zones can be detected in the zone of low resistivity value as indicated in the Fig 6. The low resistivity value in the Fig 6 due to the occurrence of the water in the pore of the soil. However, the higher resistivity value in the Fig. 6 is due to the hard rock.

In the Res Line 1, the weak zone can be found below the 32 m mark in the depth of 82 meter. However, this weak zone cannot cause the possibility of the ground movement. It is due to the zone is not available at the slope furthermore the zone elevation is lower than the lowest surface there. When the rainfall occur in the area, the weak zone detected in the resistivity data will save the water. As the result, the weight of the ground mass will increase drastically due to the present of water in the pore. In wet climates, such as in the study area, the climate factor that affects landslides is rain. The amount of rainfall, intensity and distribution of rain determine the strength of the dispersion (Shuai et al., 2016; Loredana, et al., 2017;)

In the Res Line 2, the resistivity shows that there is no possibility of the weak soil zone, infat the relatively higher resistivity value can be found at the depth below than 75 m above mean sea level. In the Res Lone 3, relatively low resistivity value of about 300 ohm.m is the possibility of weak soil zone. However the thickness of the soil is just less than 2 meter. That means, the possibility of weak zone is also can not be found here.

In the geoelectrical resistivity survey of line 3, the resistivity model shows a relatively lower resistivity value at the surface until the depth of less than 2 meter from the surface. Below that, the resistitiy value is relatively higher that is indicating the hard rock material. Generally in this resistivity line 3 model, the slope is relative stabil and there is no indication of the weak soil zone.

In the resistivity survey of Line 4, almost of all zones are the low resistivity at the surface and until 2 meter depth. The soil grain size distribution data shows that the low resistivity value consits clay and silt. However, at this zone, the sand is highest value if compare than the other lower resistivity value in all the soil sample. However, based on the height of the slope, the slope is quite gentel, so that the possibility of the weak zone can cause the landslide is almost impossible.

5. Conclusion

The investigation of the weak soil zone has been successfully done in the slope area of the hot spring tourism location, Rokan Hulu, Indonesia. The geoelectrical resistivity models show that there are some zones with relatively low resistivity value. The low resistivity value is indicating that the soil has the relatively porous so that it is possible to accommodate water. The weak zone has been found in all the geoelectrical resistivity models. However, the thickness of the weak soil zone is relatively thin taht are laying on the hard

rock material. Thus, these weak soil zone are predicted can not cause any ground movement in the future.

Acknowledgment

This research is part of the Geothermal Investigation research funding under DRPM Decentralization of Institute of Research and Community Services Universitas Riau. Thank you to all the crew members that have helped in the data acquisition.

References

- Federico, D.T., Teresa, N., Andrea, C., Lorenzo, S., 2018. Tracking morphological changes and slope instability using spaceborne and ground-based SAR data. *Geomorphology*, 300, 95-112. Doi: 10.1016/j.geomorph.2017.10.023
- Geotomo, 2007, Rapid 2-D Resistivity & IP inversion using the least-squares method. GEOTOMO SOFTWARE RES2DINV ver. 3.56. Malaysia. www.geoelectrical.com
- Islami, N., Irianti M., Nor M., 2018a. Geophysical survey for groundwater potential investigation in peat land area, Riau, Indonesia. *IOP Conference Series: Earth and Environmental Science*. 144 (1), 012001. doi: 10.1088/1755-1315/144/1/012001
- Islami, N., Taib, S.H., Yusoff, I., Ghani, A.A., 2018b. Integrated geoelectrical resistivity and hydrogeochemical methods for delineating and mapping heavy metal zone in aquifer system. *Environmental earth sciences*, 77 (10), 383. Doi: 10.1007/s12665-018-7574-4
- Jie, D., Mingsheng, L., Qiang, X., Lu, Z., Minggao, T., Jianya, G., 2018. Detection and displacement characterization of landslides using multi-temporal satellite SAR interferometry: A case study of Danba County in the Dadu River Basin. *Engineering Geology*, 240, 95-109. doi: 10.1016/j.enggeo.2018.04.015
- Loredana, A., Roberto, C., Francesco, D.P., Francesco, M., 2017. Geo-hydrological risk perception: A case study in Calabria (Southern Italy), *International Journal of Disaster Risk Reduction*, 25, 301-311. Doi: 10.1016/j.ijdrr.2017.09.022
- Margherita, C.S., Andrea, W., Vincenzo, P., Lisa, B., Anne, M., Monica, G., 2018. Forensic investigations of the CimaSalti Landslide, northern Italy, using runout simulations. *Geomorphology*, 318, 172-186. doi: 10.1016/j.geomorph.2018.04.013.
- Rock, N.M.S., Aldis, D.T., Aspden, J.A., Clarke, M.C.G., Djunuddin, Kartawa, W., Miswar, Thompson, S.J., Whandoyo, R., 1983. *Geologic Map of the Lubuksikaping Quadrangle, Sumatra*. Geological Research and Development Center, Indonesia.
- Satoru, K., Hidehisa, N., Sei-ichi, Y., Naoya, I., Tomoyuki, O., 2015. Large deep-seated landslides controlled by geologic structures: Prehistoric and modern examples in a Jurassic subduction-accretion complex on the Kii

- Peninsula, central Japan. *Engineering Geology*, 186, 44-56. Doi: 10.1016/j.enggeo.2014.10.018
- Shuai, Z., Qiang, X., Zeming, H., 2016. Effects of rainwater softening on red mudstone of deep-seated landslide, Southwest China. *Engineering Geology*, 204, 1-13. Doi: 10.1016/j.enggeo.2016.01.013
- Telford, W.M., Geldart, L.P., Sheriff, R.E., 1990. *Applied Geophysics*, 2nd Edition, Cambridge University.
- Xuanmei, F., Weiwei, Z., Xiujun, D., Ceesvan, W., Qiang, X., Lanxin, D., Qin, Y., Runqiu, H., Hans-Balder, H., 2018. Analyzing successive landslide dam formation by different triggering mechanisms: The case of the Tangjiawan landslide, Sichuan, China. *Engineering Geology*, 243, 128-144.
- Zbigniew, B., 2018. Identification of flysch landslide triggers using conventional and 'nearly real-time' monitoring methods – An example from the Carpathian Mountains, Poland. *Engineering Geology*, 244, 41-56. doi: 10.1016/j.enggeo.2018.07.012.



© 2016 Journal of Geoscience, Engineering, Environment and Technology. All rights reserved. This is an open access article distributed under the terms of the CC BY-SA License (<http://creativecommons.org/licenses/by-sa/4.0/>).